Optimization of NQR Pulse Parameters using Feedback Control

J. L. Schiano, A. J. Blauch, and M. D. Ginsberg[a]

Department of Electrical Engineering, The Pennsylvania State University,
227D Electrical Engineering West, University Park, PA 16802, USA
[a] United States Army Construction Engineering Research Laboratories,
PO Box 9005, Champaign, IL 61826, USA

Reprint requests to Prof. J. L. S.; Fax: (814) 865-7065; E-mail: schiano@steinmetz.ee.psu.edu

Z. Naturforsch. **55 a,** 67–73 (2000); received August 28, 1999

Presented at the XVth International Symposium on Nuclear Quadrupole Interactions, Leipzig, Germany, July 25 - 30, 1999.

A new method for increasing the probability of detecting nuclear resonance signals is demonstrated experimentally. It is well known that the detection of signals with a low signal to noise ratio (SNR) results in missed detections of false alarms. In situations where the noise is correlated or where limited data is averaging, it may not be possible to achieve a desired SNR through averaging alone. We present an alternative approach in which a feedback algorithm automatically adjusts pulse parameters so that the SNR and probability of correct detection are increased. Experimental results are presented for the detection of ^{14}N NQR signals.

Key words: Nuclear Quadrupole Resonance; Feedback Control; Receiver Operating Characteristics.

1. Introduction

Nuclear quadrupole resonance (NQR) provides a noninvasive means of detecting explosives [1] and narcotics [2] by revealing the presence of ^{14}N. Although ^{14}N is essentially 100% abundant, the small zero-field NQR splitting results in a low signal-to-noise ratio (SNR) that leads to missed detections and false alarms. The SNR of NQR measurements is determined by both the statistical properties of the noise and the selection of pulse sequence parameters. The standard approach to improving the SNR uses multipulse sequences that facilitate coherent signal averaging [3 - 5]. Averaging methods improve the SNR by reducing the variance of the noise, but do not increase the magnitude of the NQR signal [6]. The correlation of the noise sources limits the minimum noise variance, and hence maximum SNR, that can be achieved through averaging [7].

In conjunction with signal averaging, we propose another method which further improves the SNR of NQR measurements. The NQR signal strength depends on the amplitude, frequency, duration and repetition rate of the applied RF pulses. In most situations, these parameters are chosen before the experiment and remain unchanged during the pulse sequence. The selection of pulse parameters is based on the expected response of the experiment. In applications such as the detection of explosives using NQR, the optimal selection of RF parameters requires knowledge that is not available in practice, such as the location of the explosive with respect to the search coil and the temperature of the explosive [8]. Existing NQR detection systems sacrifice signal intensity by using fixed pulse parameters. We demonstrate that feedback control provides a means for automatically adjusting multiple pulse parameters so that the maximum NQR signal strength is obtained.

In the proposed method based on feedback control, measurements of the NQR response between RF pulses are used to optimize the pulse parameters in real-time. The feedback algorithm adjusts the pulse parameters to produce the largest possible NQR signal. We demonstrate that feedback can be used to maximize the SNR of NQR measurements by simultaneously tuning both the pulse width and offset

0932–0784 / 00 / 0100–0067 $ 06.00

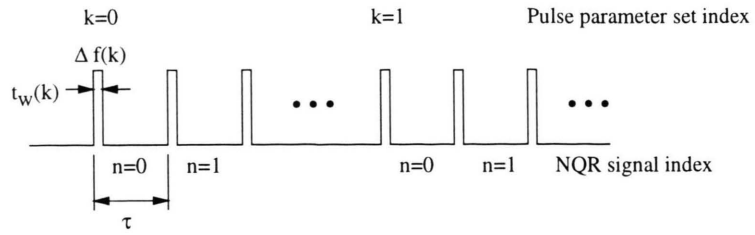

Fig. 1. SORC pulse sequence notation.

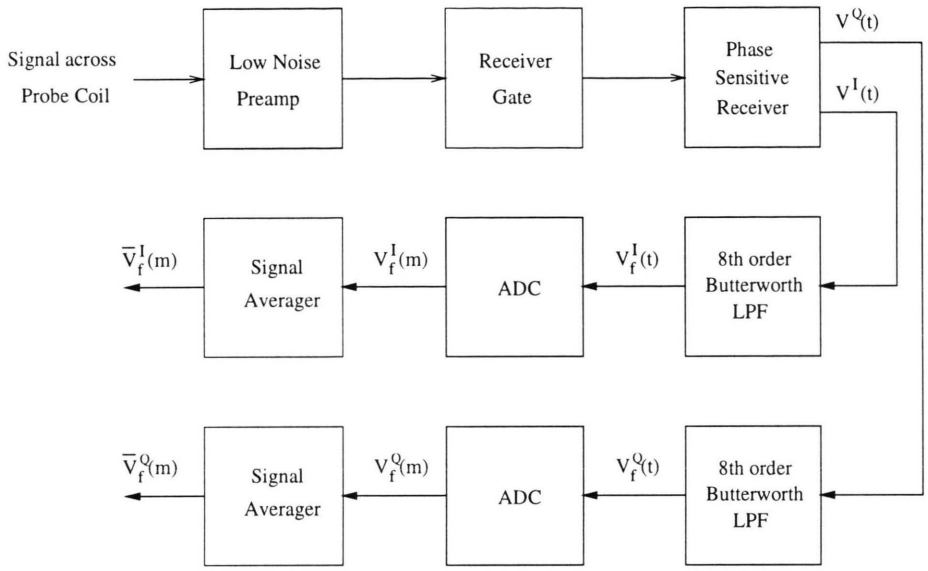

Fig. 2. Block diagram of the receiver and data acquisition system.

frequency in the strong off-resonant comb (SORC) sequence. Within the framework of signal detection theory, we also show that feedback can improve the receiver operating characteristics in detection experiments by increasing the probability of a correct detection.

2. Dual Parameter Optimization

NQR signals are generated using the SORC sequence which is a periodic series of identical RF pulses with pulse width t_w and pulse separation τ [9]. The frequency of the RF pulses is offset Δf Hz above the transition frequency ν_-. As the sequence progresses, the NQR signal observed between the RF pulses reaches a steady-state waveform. The advantage of the SORC sequence is that the signals obtained are comparable in magnitude to the FID obtained from a fully relaxed system.

In a conventional SORC sequence the pulse parameters are fixed. In this study, however, the pulse width and offset frequency are adjusted during application of the sequence. We use the notation shown in Fig. 1 to represent changes in pulse parameters. The index k is used to reference the pulse parameter set, with each k corresponding to a different set of parameter values. Individual NQR signals are indexed by n, with $n = 0$ corresponding to the first signal after the start of a new set of pulse parameters.

Figure 2 shows the general block diagram of the receiver and data acquisition system. The phase-sensitive receiver mixes the gated signal induced in the probe coil with the excitation frequency $\nu_- + \Delta f$, where Δf is the applied offset frequency above resonance. To avoid ringing in the receiver following

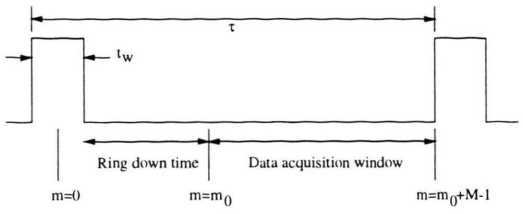

Fig. 3. Data acquisition window between RF pulses.

the application of an RF pulse, there is a 240 μs delay between the end of the RF pulse and when the receiver is turned on. The in-phase $V^{\mathrm{I}}(t;k)$ and quadrature $V^{\mathrm{Q}}(t;k)$ components of the receiver output are passed through identical 8th-order Butterworth lowpass filters with a cutoff frequency of 20 kHz to produce $V_f^{\mathrm{I}}(t;k)$ and $V_f^{\mathrm{Q}}(t;k)$, respectively. The signals $V_f^{\mathrm{I}}(m;k)$ and $V_f^{\mathrm{Q}}(m;k)$ are obtained by sampling the filtered signals at 100 kHz. The sampled signals are then sent to point-by-point signal averagers to form the averages $\bar{V}_f^{\mathrm{I}}(m;k)$ and $\bar{V}_f^{\mathrm{Q}}(m;k)$ for N SORC signals. The data acquisition window between RF pulses in shown in Figure 3.

A wide variety of signal metrics are available for quantifying the amplitude of the SORC waveform, including peak-to-peak voltage, mid-signal amplitude, signal energy, and peak spectral magnitude. For this paper, we choose the SORC signal power as the feedback metric for tuning the SORC pulse parameters [10], and for fixed pulse parameters $t_w(k)$ and $\Delta f(k)$ is given by

$$P(k) = \frac{1}{M} \sum_{m=m_0}^{m_0+M-1} \left(\bar{V}_f^{\mathrm{I}}(m;k) - V_{\mathrm{DC}}\right)^2, \quad (1)$$

where V_{DC} is the DC offset measured at the filter output in the absence of an NQR signal.

Methods for separately optimizing the pulse width and offset frequency have been previously demonstrated [10, 11]. The dual tuning algorithm presented here is an extension of this earlier work. A gradient ascent algorithm maximizes the performance index

$$J(t_w(k), \Delta f(k)) = J(k) = P(k) \quad (2)$$

by adjusting the pulse width $t_w(k)$ and offset frequency $\Delta f(k)$. The power $P(k)$ is calculated from the steady-state SORC waveform produced by fixing the pulse parameters $t_w(k)$ and $\Delta f(k)$. After a period of fifteen hundred RF pulses, N consecutive steady-state SORC signals are acquired and coherently added to form an average SORC signal $\bar{V}_f^{\mathrm{I}}(m;k)$ from which the power metric $P(k)$ is determined.

The pulse width $t_w(k)$ and offset frequency $\Delta f(k)$ are updated using the rules

$$t_w(k+1) = t_w(k) + \lambda_{t_w}(k) \nabla_{t_w} J(k-1), \quad k = 2, 4, 6, \cdots, \quad (3)$$

$$\Delta f(k+1) = \Delta f(k) + \lambda_{\Delta f} \nabla_{\Delta f} J(k-1), \quad k = 3, 5, 7, \cdots. \quad (4)$$

The pulse parameters $t_w(0)$, $t_w(1)$, $\Delta f(0) = \Delta f(1)$, and $\Delta f(2)$ are initial values that are specified before the pulse sequence is started. The gradients $\nabla_{t_w} J(k-1)$ and $\nabla_{\Delta f} J(k-1)$ are approximated as [10, 11]

$$\nabla_{t_w} J(k-1) = G(J(k-1) - J(k-2)) \cdot G(t_w(k-1) - t_w(k-2)), \quad (5)$$

$$\nabla_{\Delta f} J(k-1) = G(J(k-1) - J(k-2)) \cdot G(\Delta f(k-1) - \Delta f(k-2)), \quad (6)$$

where

$$G(x) = \begin{cases} 1 & x \geq 0, \\ -1 & x < 0. \end{cases} \quad (7)$$

The gradients $\nabla_{t_w} J(k)$ and $\nabla_{\Delta f} J(k)$ can only take on values of ± 1. The sign determines the direction in which the parameter should be incremented in order to increase the signal metric. The learning factors $\lambda_{t_w}(k)$ and $\lambda_{\Delta f}$ determine the magnitude of the change in pulse parameters. When tuning pulse width, it is useful to start with a large learning factor so that the algorithm rapidly homes in on the optimal pulse width [11]. However, to avoid a limit cycle oscillation with a large radius about the optimal pulse width, the learning factor is decremented as follows

$$\lambda_{t_w}(k) = \begin{cases} 20\ \mu\mathrm{s} & k = 0, 2, \cdots, 8, \\ 15\ \mu\mathrm{s} & k = 10, 12, \cdots, 18, \\ 10\ \mu\mathrm{s} & k > 20. \end{cases} \quad (8)$$

A fixed learning factor $\lambda_{\Delta f} = 50$ Hz is used for tuning the offset frequency [10].

Because the gradients in (5) and (6) are always non-zero, the gradient algorithm converges to a limit cycle instead of a single point. The parameters are

tuned for a fixed number of iterations which is chosen sufficiently large so that the algorithm converges to a limit cycle.

3. Receiver Operating Characteristics

Binary signal detection theory [12] is a useful tool for studying the effect of signal averaging and feedback on the detection of nuclear resonance signals in noise. The binary detection system in Fig. 4 can be used to represent a NQR detection system. In this context the state s_1 represents the presence of a material that produces a NQR signal, while s_0 represents the absence of the material. The received signal $r(t)$ is a combination of the source signal $s(t)$ and noise from the channel. By observing $r(t)$, the receiver must decide whether the source is in state s_0 or s_1. This decision is accomplished in two stages. First, a signal processing unit transforms the received signal $r(t)$ into a scalar metric $\Lambda(r)$. Second, a threshold detector compares $\Lambda(r)$ to a threshold Γ to decide whether or not a NQR signal is present

$$\hat{s} = \begin{cases} s_0, & \Lambda(r) < \Gamma \\ s_1, & \Lambda(r) \geq \Gamma. \end{cases} \tag{9}$$

The function $\Lambda(r)$ and the threshold value Γ are chosen by the designer.

The probability of correct detection P_d and probability of false alarm P_f are used to characterize the detection system. As an illustration, Fig. 5 shows a normal probability density function $\mathcal{N}(\mu, \sigma^2)$ with mean μ and variance σ^2 for the two different states of the source. The mean is determined by the state of the source, $\mu = 0$ for $s = s_0$ and $\mu = d$ when $s = s_1$. The variance σ^2 is assumed identical for both states of the source. The probability of a correct detection P_d is the light gray area under the density function $\mathcal{N}(d, \sigma^2)$ for $\Lambda(r) \geq \Gamma$. Similarly, the probability of a false alarm P_f is the dark gray area under the density function $\mathcal{N}(0, \sigma^2)$ for $\Lambda(r) \geq \Gamma$. In explosives detection a fixed threshold value is used, and its value is chosen to limit the probability of a false alarm. Ideally, we would like P_f

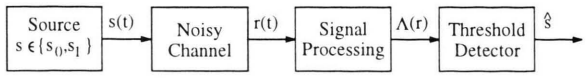

Fig. 4. Block diagram of a binary signal detection system.

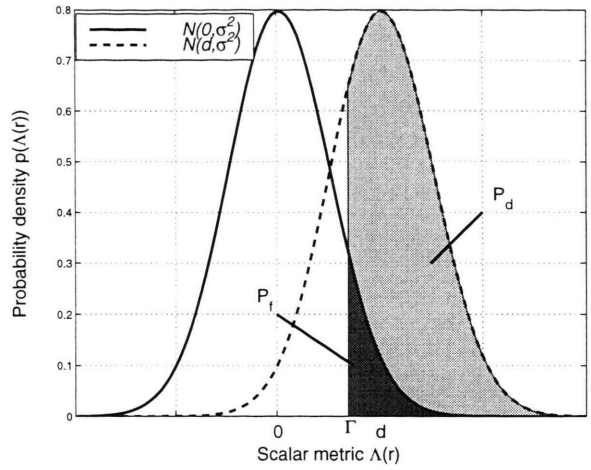

Fig. 5. Probability density functions of $\Lambda(r)$ for $s = s_0$ and $s = s_1$.

and P_d to be as close as possible to 0 and 1, respectively.

In signal detection applications it is often assumed that the signal $s_1(t)$ is fixed, resulting in a signal metric with a constant mean d. In nuclear resonance experiments this assumption can be lifted, because the experimenter can influence the magnetization signal by varying the pulse sequence parameters. From Fig. 5, increasing d shifts the probability density function $\mathcal{N}(d, \sigma^2)$ to the right, thereby raising the probability of correct detection P_d for a fixed Γ. On the other hand,with Γ fixed, increasing d has no effect on the dark gray area which determines the probability of a false alarm.

The performance of a dection system is characterized using a receiver operating charateristic (ROC) curve which is a two-dimensional plot of the probabilities P_d and P_f. Each point on the curve corresponds to a fixed threshold Γ. By varying Γ we move along the ROC curve. In Sect. 4 we show how feedback effects the ROC curve.

4. Experimental Results

The experiments were performed using a 50 g sample of sodium nitrite at room temperature near the $\nu_- = 3.6$ MHz transition. The ν_- transition is dominated by a single spin-lattice relaxation time $T_{1\ell}$ which was measured using the method of progressive saturation. The spin-spin relaxation time T_2 was measured using a two-pulse spin-echo decay. These time constants are estimated as 0.3 s and 6 ms,

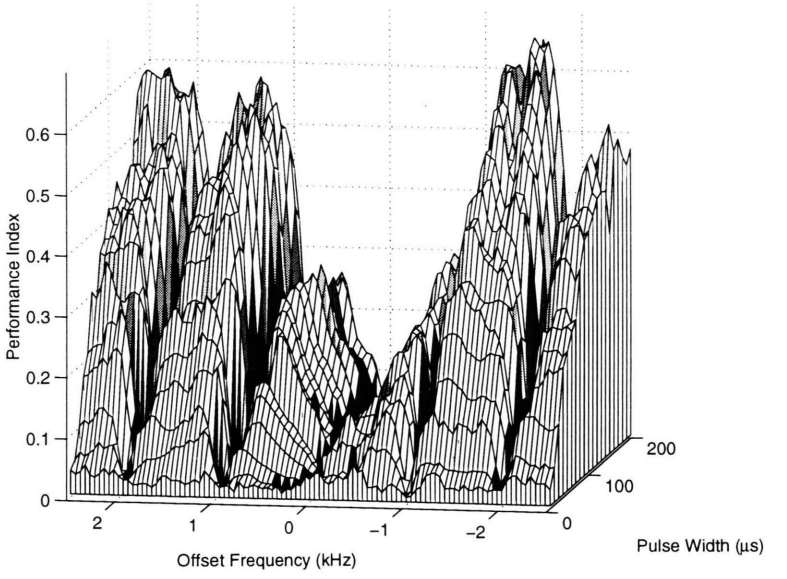

Fig. 6. Performance index as a function of pulse width and offset frequency.

respectively. The T_2^* line-shape parameter was determined from the spin-echo decay, and is approximately 1 ms.

A custom-made 1 kW pulsed spectrometer was used in the experiments [13]. This system can acquire data, perform calculations, and update pulse parameters in real-time. The quality factor of the probe coil is approximately 150. The amplitude of the applied RF pulses is fixed so that the magnetic field amplitude at the coil center is approximately 5 Gauss. The corresponding output power of the transmitter is approximately 25 Watts. In all experiments, the pulse separation was fixed at 1 ms.

The power of the SORC waveform is used as a metric, or performance index, in determining the optimality of pulse parameters. The dependence of the performance index on pulse width and offset frequency is shown in Figure 6. With the pulse width held constant, the steady-state SORC signal was recorded for offset frequencies ranging from –2.5 kHz to 2.5 kHz in 50 Hz steps. This experiment was repeated for pulse widths ranging from 10 μs to 200 μs in 10 μs steps. For each pulse width and offset frequency, two thousand steady-state SORC signals were filtered and averaged. The performance index for a given pair of pulse parameters represents the power of the average waveform. Consistent with the results reported by Marino [9, 14], the SORC signal intensity can vary widely as a function of pulse parameters.

The ability of the dual tuning algorithm to maximize the signal metric $P(k)$ is shown in Figure 7. In this experiment $N = 36$ signals were averaged to improve the SNR. The initial pulse width and offset frequencies are chosen as $t_w(0) = 20$ μs, $t_w(1) = 40$ μs, $\Delta f(0) = \Delta f(1) = 0$ Hz, and $\Delta f(2) = 50$ Hz respectively. The actual offset frequency was unknown due to temperature variations of the sample. With no sample present, the performance index remains unchanged, and provides a graphical representation of the noise floor. With a sample present, the dual tuning algorithm increased the performance index well above the noise floor.

The effect of feedback on the ROC curve was determined by performing a series of two hundred experiments, half with the sample present and half with the sample absent. For each experiment, the performance index is compared against the threshold Γ to decide whether or not a sample is present. Let N_c (N_f) represent the number of experiments where the sample is present (absent) and the signal metric is larger than Γ. The probabilities of correct detection and false alarm are then calculated as $N_c/100$ and $N_f/100$. The ROC curve is generated using one hundred values of Γ ranging from 0 to 1 in 0.01 steps.

The ROC curves in Fig. 8 show the effect of feedback on the detection of an NQR signal. The solid curve is obtained with a fixed set of pulse parameters. The dashed and dotted ROC curves are obtained after the control algorithm tunes the pulse parameters

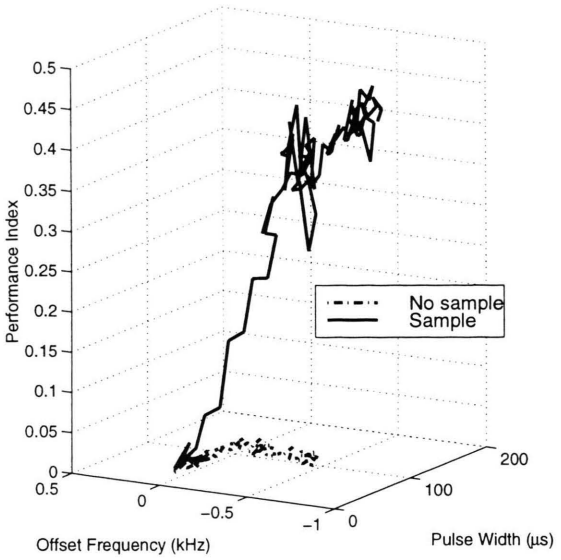

Fig. 7. Tuning history when the SORC signal metric is based on the average of $N = 36$ SORC signals.

using 20 and 80 iterations, respectively. As predicted, the feedback algorithm increases the probability of correct detection, but does not change the probability of false alarm.

5. Conclusions

We successfully demonstrated that a gradient tuning algorithm can automatically adjust two pulse parameters so that the amplitude of the nuclear resonance signal is increased. The effect of feedback on the receiver operating characteristic curve of an NQR

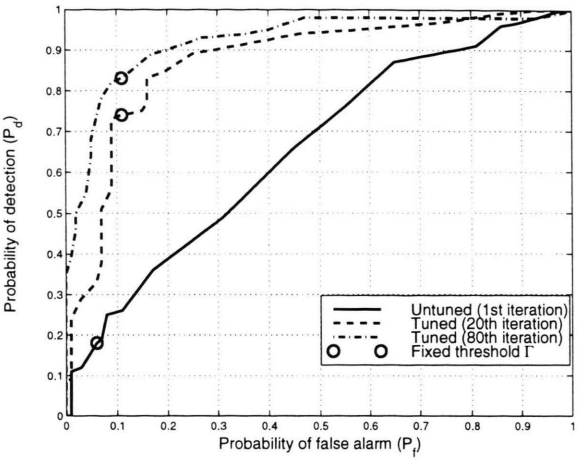

Fig. 8. Receiver operating characteristics for tuned and untuned pulse parameters.

detection system was investigated. As a result of the increased signal amplitude, the probability of correct detection was increased. These results are also applicable to other nuclear resonance detection systems, for example, the detection of subterranean water using nuclear magnetic resonance [15]. The use of feedback to improve the ROC curve in nuclear resonance detection systems is likely to be useful in situations where the pulse parameter values that yield the largest signal amplitude are initially unknown.

Acknowledgements

This work was funded in part by the United States Army Construction Engineering Research Laboratories under contract DACA 88-95-K-0002.

[1] T. Hirschfeld and S. M. Klainer. J. Mol. Structure **58**, 63 (1980).

[2] J. P. Yesinowski, M. L. Buess, A. N. Garroway, M. Ziegeweid, and A. Pines. Analyt. Chem. **67**, 2256 (1995).

[3] M. L. Buess, A. N. Garroway, and J. B. Miller. J. Magn. Resonance **92**, 348 (1991).

[4] R. A. Marino and S. A. Klainer. J. Chem. Physics **67**, 3388 (1977).

[5] D. Y. Osokin. J. Mol. Structure **83**, 243 (1982).

[6] M. P. Klein and G. W. Barton. Rev. Sci. Instruments **34**, 754 (1963).

[7] R. R. Ernst. Rev. Sci. Instruments **36**, 1689 (1965).

[8] A. D. Hibbs, G. A. Barrall, P. V. Czipott, D. K. Lathrop, Y. K. Lee, E. E. Magnuson, R. Matthews, and S. A. Vierkotter. Landmine detection by nuclear quadrupole resonance. In Abinash C. Dubey, James F. Harvey, and Thomas Broach, editors, Detection and Remediation Technologies for Mines and Minelike Targets III, 1998, vol. 3392. p. 522-532.

[9] S. S. Kim, J. R. P. Jayakody, and R. A. Marino. Z. Naturforsch. **47a**, 415 (1992).
[10] A. J. Blauch, J. L. Schiano, and M. D. Ginsberg. J. Magn. Resonance **139**, 139 (1999).
[11] J. L. Schiano, T. Routhier, A. J. Blauch, and M. D. Ginsberg. J. Magn. Resonance **140**, 84. (1999).
[12] R. N. McDonough and A. D. Whalen. Detecion of Signals in Noise, 2nd ed., San Diego 1995.
[13] J. L. Schiano and M. D. Ginsberg. Z. Naturforsch. **55a**, 61 (2000).
[14] R. A. Marino, S. M. Klainer, and T. Hirschfeld. Fourier transform nuclear quadrupole resonance spectroscopy. In: Fourier, Hadamard, and Hilbert Transforms in Chemistry, pages 147-182. Plenum Press, New York 1982.
[15] A. V. Legchenko and O. A. Shushakov. Geophysics **63**, 75 (1998).